



Influence of crustal cumulates on ^{210}Pb disequilibria in basalts

James A. Van Orman ^{a,*}, Alberto E. Saal ^b

^a Department of Geological Sciences, Case Western Reserve University, Cleveland, OH 44106, USA

^b Department of Geological Sciences, Brown University, Providence, RI 02912, USA

ARTICLE INFO

Article history:

Received 5 February 2009

Received in revised form 22 April 2009

Accepted 24 April 2009

Available online 20 May 2009

Editor: R.W. Carlson

Keywords:

uranium decay series

midocean ridge

U-series

radioactive disequilibrium

diffusive fractionation

ABSTRACT

In historical basalts from a wide range of tectonic settings, ^{210}Pb is often found to have an activity deficit relative to its predecessor ^{226}Ra . Several processes have been hypothesized as causes of ^{210}Pb deficits in basalts. In subduction zone and ocean island environments, ^{210}Pb deficits have often been attributed to shallow magmatic degassing. At mid-ocean ridges, ^{210}Pb deficits have been inferred to result from mantle melting, limiting the time between melt production and eruption to 100 years or less. Here we present an alternative mechanism for producing ^{210}Pb deficits in magmas, by diffusive exchange between a melt and cumulate minerals (plagioclase and/or clinopyroxene) in the crust. The deficit in ^{210}Pb develops in response to its decay toward secular equilibrium with ^{226}Ra within the mineral grains; decay provides an internal sink for ^{210}Pb that drives continuous diffusive exchange with the melt. Deficits in ^{210}Pb develop under a broad range of conditions, in enriched and depleted melts and during interaction with young or old cumulate minerals. The magnitude of the deficit depends mainly on the equilibrium mineral/melt partition coefficients for Pb and Ra and on the melt/rock ratio during diffusive interaction, and is only weakly dependent on the relative diffusivities of Ra and Pb in the minerals or the trace element disequilibrium between the melt and cumulate minerals. Plagioclase in the crust has greater leverage on the ^{210}Pb – ^{226}Ra system than any silicate mineral present during mantle melting, and is capable of inducing significant ^{210}Pb deficits in the melt even at melt fractions above 50%. Its influence on the melt is also rapid, with a substantial ^{210}Pb deficit developing in less than a year and approaching a steady state value after several decades or less. The strong control crustal cumulates are capable of exerting on ^{210}Pb – ^{226}Ra fractionation in melts indicates that they may have a significant role in a wide range of tectonic environments, and suggests caution in interpreting ^{210}Pb deficits as a signature of mantle melting, or as a product of ^{222}Rn degassing.

© 2009 Elsevier B.V. All rights reserved.

1. Introduction

The ^{238}U decay series includes a number of intermediate nuclides that have proven useful in constraining the processes and timing of melt generation, differentiation and transport in Earth's mantle and crust. In a region of mantle or crust that has remained closed for $\sim 10^6$ years the decay series reaches a steady state, known as secular equilibrium, in which the activities of all intermediate daughter nuclides are equal to that of the parent. During partial melting, or any other process that leads to chemical fractionation among the members of the decay chain, the steady state is disrupted and the activities of all members of the chain are no longer equal. Following such an event, an intermediate daughter returns to secular equilibrium with its predecessor on a timescale governed by its decay rate. Secular disequilibria involving the relatively long-lived intermediate nuclides ^{230}Th ($t_{1/2} = 75,000$ yr) and ^{226}Ra ($t_{1/2} = 1600$ yr) have received the most attention, and have provided many important constraints on mantle melting parameters (e.g. McKenzie,

2000; Bourdon and Sims, 2003; Lundstrom, 2003). Radioactive disequilibria involving ^{210}Pb , with a half-life of only 22 years, have been measured less frequently but have the potential to yield tighter bounds on rates of magma generation and transport, provided that the processes creating secular disequilibrium are known.

Disequilibrium ($^{210}\text{Pb})/(^{226}\text{Ra})$ activity ratios have been reported in recently erupted volcanic rocks associated with subduction zones (Oversby and Gast, 1968; Rubin et al., 1989; Gill and Williams, 1990; Condomines et al., 1995; Gauthier and Condomines, 1999; Turner et al., 2004), intraplate oceanic islands and seamounts (Oversby and Gast, 1968; Rubin and Macdougall, 1989; Rubin et al., 2005; Sigmarsson et al., 2005; Reagan et al., 2008; Sims et al., 2008) and mid-ocean ridges (Sigmarsson, 1996; Rubin et al., 2005; Bergmanis et al., 2007). In all tectonic settings, most volcanic samples that exhibit ^{210}Pb disequilibrium have $(^{210}\text{Pb})/(^{226}\text{Ra}) < 1$, referred to here as a ^{210}Pb deficit. Partial melting of the mantle is capable of creating a ^{210}Pb deficit in basalts, because the solid/melt partition coefficient for Pb is greater than for Ra (Blundy and Wood, 2003). Shallow magmatic differentiation processes also are able to produce ^{210}Pb deficits. Crystallization of plagioclase or Fe–Ni sulfide, both of which preferentially incorporate Pb, and degassing of ^{222}Rn , a short-lived ($t_{1/2} = 3.8$ days) precursor to ^{210}Pb in the ^{238}U

* Corresponding author.

E-mail addresses: james.vanorman@case.edu (J.A. Van Orman), Alberto_Saal@brown.edu (A.E. Saal).

decay chain, may produce a ^{210}Pb deficit in the melt. Long-term degassing has been suggested as the cause of ^{210}Pb deficits in ocean island lavas (Rubin and Macdougall, 1989) and in subduction zone lavas (Gauthier and Condomines, 1999; Turner et al., 2004). At mid-ocean ridges, however, ^{210}Pb deficits are not readily attributed to shallow magmatic differentiation processes. In the Vestmannaeyjar volcanic system in Iceland the largest ^{210}Pb deficits are found in the least differentiated lavas (Sigmarsson, 1996). Similarly, in mid-ocean ridge basalts from the Juan de Fuca ridge and East Pacific Rise, ^{210}Pb deficits are greatest in the least differentiated samples, and the deficits are anti-correlated with geochemical indices of plagioclase and sulfide fractionation (Rubin et al., 2005). ^{210}Pb deficits in these samples are also correlated with ^{226}Ra excesses, which are often interpreted to be generated during mantle melting. These correlations led Rubin et al. (2005) to conclude that ^{210}Pb deficits in these samples were likely produced by partial melting in the mantle. If so, this would place an upper limit of ~100 years on the time between melt production, at tens of kilometers depth, and eruption at the surface.

Such rapid melt transport is not easy to reconcile with physical considerations. Because members of the ^{238}U decay series are highly incompatible in the minerals present during mantle melting, and thus quickly lost to the melt when melting takes place in local equilibrium, they are likely to be fractionated significantly only when the melt fraction is small, and when melt is distributed in grain-scale porous networks. Flow in such fine networks is far too slow to deliver ^{210}Pb disequilibria to the surface within the required timeframe of 100 years or less (Richardson and McKenzie, 1994; Kelemen et al., 1997). Coarser melt channels are capable of transporting melt at sufficient rates (e.g. McKenzie, 2000); however, time is required to gather melts from the grain-scale porous networks in which U-series disequilibria are produced into the much coarser channel networks required for rapid transport, and although this time is not well constrained it appears unlikely to be short enough to allow ^{210}Pb deficits to survive. Hart (1993) hypothesized a fractal root system to transfer melts from grain-scale networks to high-velocity channels, but even in this highly efficient hypothetical system it appears difficult to move melts from the grain scale, where Pb and Ra are fractionated, to high-speed channels within less than 100 years.

A possible alternative mechanism for creating $(^{210}\text{Pb})/(^{226}\text{Ra})$ disequilibrium is through the diffusive interaction of melts with cumulate minerals in the crust. Saal and Van Orman (2004) and Van Orman et al. (2006) showed that diffusive exchange with plagioclase and/or clinopyroxene cumulates could significantly fractionate ^{226}Ra and ^{230}Th . During diffusive exchange, either an excess or a deficit in ^{226}Ra can be produced, depending on the incompatible trace element enrichment of the melt relative to that of a melt in partitioning equilibrium with the cumulate. A relatively depleted melt absorbs both ^{226}Ra and ^{230}Th from cumulate minerals, with ^{226}Ra entering the melt more rapidly due to its higher (estimated) diffusivity, thus producing excess ^{226}Ra in the melt. A relatively enriched melt, on the other hand, in general loses ^{226}Ra and ^{230}Th to the cumulate minerals, and develops a ^{226}Ra deficit, again due to the more rapid diffusivity of Ra. Rubin et al. (2005) argued that diffusive exchange with cumulates in the crust is unlikely to lead to ^{210}Pb deficits under the same conditions that lead to ^{226}Ra excesses, and is therefore unlikely to explain the negative correlation between $(^{210}\text{Pb})/(^{226}\text{Ra})$ and $(^{226}\text{Ra})/(^{230}\text{Th})$ in mid-ocean ridge basalts from Juan de Fuca and the East Pacific Rise. In plagioclase, Pb, Ra and Th are all incompatible and the diffusion coefficients are expected to decrease in the order $D_{\text{Pb}} > D_{\text{Ra}} > D_{\text{Th}}$ (Saal and Van Orman, 2004). Therefore, it is argued that interaction of a relatively depleted melt with plagioclase would produce both ^{226}Ra and ^{210}Pb excesses in the melt, while interaction of an enriched melt with plagioclase would lead to deficits in both (Rubin et al., 2005). In clinopyroxene, on the other hand, Pb and Ra are expected to diffuse at similar rates and hence it is argued that clinopyroxene would not alter significantly the $(^{210}\text{Pb})/(^{226}\text{Ra})$ activity ratio in the melt (Rubin et al., 2005).

An implicit premise of these arguments is that the behavior of ^{210}Pb during diffusive interaction can be approximated without considering its simultaneous radioactive production and decay. The behavior of ^{210}Pb during diffusive interaction between melt and cumulate minerals is significantly different from that of ^{226}Ra due to its much faster rate of decay. The rapid decay of ^{210}Pb provides a substantial driving force for diffusive exchange and hence cannot be treated separately from diffusion. In this paper we show that diffusion induced by the adjustment of ^{210}Pb toward secular equilibrium with ^{226}Ra is a primary control on changes in the $(^{210}\text{Pb})/(^{226}\text{Ra})$ activity ratio when melts interact with minerals. Regardless of the relative enrichment of the interacting melt or the precise values of the diffusion coefficients, we find that the $(^{210}\text{Pb})/(^{226}\text{Ra})$ activity ratio in the melt drops significantly during diffusive interaction with plagioclase and/or clinopyroxene cumulates.

2. Model

The objective of the simple modeling presented here is to investigate the influence of diffusive interaction with cumulate minerals on the ^{210}Pb – ^{226}Ra activity ratio of a melt that is passing through the crust. For this purpose, we use the finite difference model presented by Van Orman et al. (2006) to calculate the evolution with time of (^{238}U), (^{230}Th), (^{226}Ra) and (^{210}Pb) in an idealized system consisting of spherical mineral grains interacting with a finite reservoir of melt that begins in secular equilibrium. Simulation results are presented both for very simple systems in which melt interacts with a single mineral, and more complicated systems that contain both plagioclase and clinopyroxene. The single-mineral simulations are even simpler than those modeled by Saal and Van Orman (2004), in that the melt is assumed to be in trace element partitioning equilibrium with the minerals; i.e. the long-lived parent nuclide ^{238}U is distributed homogeneously throughout each mineral, and is in partitioning equilibrium with the melt. These single-mineral simulations, although far simpler than diffusive interactions that are likely to take place under natural conditions, provide a useful illustration of the controls on ^{210}Pb – ^{226}Ra fractionation during melt–cumulate interaction. The more complicated two-mineral simulations are similar to those presented in Van Orman et al. (2006), and involve interactions with melts that are both more enriched and more depleted than a melt in partitioning equilibrium with the cumulate minerals. In all cases, diffusive interaction is assumed to take place at constant temperature and pressure, with constant diffusion and partition coefficients (Table 1).

Table 1
Partition and diffusion coefficients used in the simulations.*

	Mineral/melt partition coefficients		Diffusion coefficients (m ² /s)	
	Cpx	Plag	Cpx	Plag
U	0.018	0.0006	2.1e-21	3.1e-21
Th	0.021	0.002	3.2e-21	3.1e-21
Ra	4e-05	0.049	1.3e-18	6.9e-19
Pb	0.009	0.66	2.2e-18	2.1e-17

* The partition coefficients for U, Th and Ra are from Saal and Van Orman (2004). The value used for Ra is similar to the experimental value obtained for partitioning between anorthite and basaltic melt at 1400 °C (Miller et al., 2007). The partition coefficient for Pb between plagioclase and melt is based on the experiments and revised parameterization of Bindeman et al. (1998, 2007), and the value for clinopyroxene/melt is the average of experimental values determined by Lundstrom et al. (1994) and Salters et al. (2002). All diffusion coefficients correspond to a temperature of 1200 °C. Values for U and Th in clinopyroxene are from Van Orman et al. (1998), for diffusion parallel to the c axis, with f_{O_2} at the quartz–fayalite–magnetite buffer. The diffusion coefficient for Pb in clinopyroxene is the average of values determined by Cherniak (1998, 2001) for specimens of different composition. The diffusion coefficient for Pb in plagioclase is from Cherniak (1995), for diffusion in labradorite parallel to the c axis. Diffusion coefficients for Ra, and for U and Th in plagioclase, are estimated values from Saal and Van Orman (2004).

Throughout each simulation, partitioning equilibrium is maintained at the interface between each mineral grain and the melt, and the liquid is assumed to rehomogenize continuously. These are reasonable assumptions, since the typical equilibration time for mineral/melt interface reactions is less than a second (Zhang et al., 1989) and the diffusional homogenization time for melts residing in grain-scale porous networks is on the order of minutes (with melt tubules along mineral triple junctions having effective radii of $\sim 10 \mu\text{m}$, for 1 mm grain size and 1% porosity; Hart, 1993). The exchange of nuclides between the minerals and melt is controlled by diffusion through the minerals, in response to a concentration gradient between the mineral interior and rim that may result from initial chemical disequilibrium with the melt and/or from radioactive decay within the mineral. The differential equations that describe simultaneous diffusive exchange and radioactive decay in this idealized system are given in Van Orman et al., 2006 (their Eqs. (5)–(7)), and the corresponding finite difference equations are solved numerically using an implicit Crank–Nicolson method. At each time step in the simulation, the change in concentration of a nuclide within a radial element of the mineral grain depends on its local decay within that element, local production due to decay of its parent (except in the case of ^{238}U , which has no parent), and diffusive transfer of the nuclide to or from the adjacent radial elements. Likewise, in the melt the change in concentration of a nuclide at a given time depends on the production and decay of the nuclide within the melt and on diffusive transfers to or from each mineral.

In the simulations presented here, the mineral/melt interface is assumed to remain static; dissolution and precipitation of minerals are not considered. Although in general the melt percolating through a cumulate pile is unlikely to be in equilibrium with the minerals, dissolution and precipitation are unlikely to have a large influence on the results. For a melt fraction of a few percent or less, it can be shown through a simple mass balance argument that dissolution of clinopyroxene or plagioclase has only a small influence compared to diffusive exchange, even if the melt dissolves an amount equal to its own mass (see Saal and Van Orman, 2004, Section 3.6). Dissolution and precipitation may have more influence when the melt fraction is large; however, at very large melt fractions the cumulate minerals have little leverage on the composition of the melt, regardless of whether the exchange is controlled by diffusion or by dissolution/precipitation.

Gas and sulfide phases are not considered in the modeling presented here, although they may be important in real systems; our focus is on the effects of diffusive interaction between melts and gabbroic cumulates. Very short-lived intermediate nuclides, including ^{222}Rn , also are not considered. Instead ^{210}Pb is treated as though it were the immediate daughter of ^{226}Ra , and short-range transport by diffusion of the intermediate nuclides (including ^{222}Rn) and by alpha recoil are neglected. Including these effects would enhance the effective diffusivity of ^{210}Pb (and also of ^{230}Th and ^{226}Ra), but probably by a very small factor. Diffusional transport of ^{222}Rn during its lifetime of several days would be significant compared to ^{210}Pb diffusion on the timescales of interest only if Rn diffusion were many orders of magnitude more rapid than Pb. Alpha recoil, assuming randomly oriented jumps each with a length of 40 nm, produces transport equivalent to diffusional transport of Pb in clinopyroxene or plagioclase over a time of less than an hour. These effects, although expected to be small, can nevertheless be addressed in an approximate way by increasing the effective diffusivity of Pb. As discussed below, in Sections 3.1 and 3.2, even large variations in the diffusivity of Pb do not fundamentally alter the model results.

3. Results

3.1. Melt-clinopyroxene interaction

Two simple end-member cases of closed-system melt-clinopyroxene exchange illustrate the behavior of ^{210}Pb in this simple system. In both

cases the entire clinopyroxene crystal and melt are in partitioning equilibrium with respect to ^{238}U , but the intermediate daughters ^{230}Th , ^{226}Ra and ^{210}Pb have two different initial distributions. In the “partitioning equilibrium” case, illustrated in Fig. 1a, the intermediate daughters also begin in partitioning equilibrium with the melt, as would be the case if clinopyroxene had precipitated from the melt without undergoing any subsequent evolution (i.e. “young” clinopyroxene). In the “secular equilibrium” example (Fig. 1b), the intermediate daughters within the clinopyroxene grain begin with activities equal to that of ^{238}U , as would be the case if the clinopyroxene had evolved in chemical isolation for several hundred thousand years (i.e. “old” clinopyroxene) before beginning to interact with the same melt again. In this case, while ^{238}U is in partitioning equilibrium with the melt, its intermediate daughters within the interior of the mineral grain are far from being in partitioning equilibrium. In both examples illustrated in Fig. 1, and in most of the other examples shown in this paper, the fraction of melt in the system is 1% and the mineral grains have radii of 0.25 mm. This melt fraction is within the range inferred from seismic investigations of the crust–mantle transition zone beneath the EPR (Dunn et al., 2000, 2001; Dunn and Forsyth, 2003). Varying the melt fraction does not fundamentally change the behavior of the system, but has a strong influence on the magnitude of ^{210}Pb – ^{226}Ra fractionation; the greater the melt fraction the less leverage the mineral has on the activity ratios in the melt. The influence of variations in melt fraction on ^{210}Pb – ^{226}Ra fractionation is discussed below, in Section 3.4. Variations in the grain size are discussed near the end of this section.

Radium is much more incompatible in clinopyroxene than Pb, and Pb is slightly more incompatible than Th. Accordingly, in the “partitioning equilibrium” case shown in Fig. 1a, ^{226}Ra initially has the lowest activity in clinopyroxene and ^{230}Th the highest. With time the activity of ^{226}Ra within the interior of the clinopyroxene grain increases toward secular equilibrium with ^{230}Th , but only slightly on the timescale of 100 years considered in this simulation. Ingrowth leads to a slowly increasing core-to-rim gradient in ^{226}Ra concentration, which results in outward diffusion to the melt. While the activity of ^{226}Ra in the interior of the grain slowly rises, the activity of ^{210}Pb decreases rapidly toward secular equilibrium with ^{226}Ra . This results in an inward gradient of ^{210}Pb concentration, and hence diffusive uptake of ^{210}Pb from the melt. Thus, the ^{226}Ra activity slowly rises in the melt while the ^{210}Pb activity decreases (Fig. 1c), producing a ^{210}Pb deficit that gradually increases with time (Fig. 1d).

In the “secular equilibrium” case shown in Fig. 1b, both ^{226}Ra and ^{210}Pb begin with high activities in clinopyroxene, relative to their values at partitioning equilibrium, and thus when the simulation begins both diffuse outward to the melt. Without considering the effects of decay, the diffusive fluxes of (^{226}Ra) and (^{210}Pb) would be similar, with the slower diffusivity of Ra being compensated by its higher concentration gradient near the grain edge. However, as in the case considered above, the decay of ^{210}Pb toward secular equilibrium with ^{226}Ra has a strong influence on its behavior. At the grain edge, ^{210}Pb is constrained to be in partitioning equilibrium with the melt. Just inward of the grain edge, the activity of ^{210}Pb is depressed because it decays toward secular equilibrium with ^{226}Ra . The result is that the gradient near the edge is lower than it would be in the absence of radioactive decay, and the flux of ^{210}Pb out of the clinopyroxene is correspondingly diminished. After thirty years the concentration gradient has actually reversed its slope near the grain edge (Fig. 1b), and the transfer of ^{210}Pb from clinopyroxene to melt reverses. This happens because ^{226}Ra continuously diffuses to the melt, driven by its initial high activity in the clinopyroxene, leading to a continuously increasing ^{226}Ra activity in the melt, and a corresponding increase in ^{210}Pb in the melt due to ^{226}Ra decay (Fig. 1c). The concentration of ^{210}Pb at the clinopyroxene rim must therefore increase, to maintain partitioning equilibrium with the melt. Meanwhile, in the interior of the clinopyroxene, ^{210}Pb decays (or grows in, depending on location) toward secular equilibrium with ^{226}Ra ; this causes (^{210}Pb) to be drawn

down just inward of the interface with the melt, and this ultimately produces a reversed gradient. The net decay of ^{210}Pb within the clinopyroxene prevents (^{210}Pb) in the melt from keeping pace with (^{226}Ra) as it diffuses out of the crystal. Thus, as in the very different case considered above, interaction with clinopyroxene leads to a ^{210}Pb deficit in the melt. In the two different examples modeled here the activities in the melt evolve along quite different trajectories (Fig. 1c),

but the magnitude of the ^{210}Pb deficit produced after several decades of interaction is similar (Fig. 1d).

Simulations in which the diffusion coefficient for Pb or Ra is varied from the values shown in Table 1 demonstrate that the (^{210}Pb)/(^{226}Ra) activity ratio of the melt following diffusive interaction is not very sensitive to variations in the diffusion coefficients. This may seem counterintuitive, but results from the strong control of ^{210}Pb decay on its diffusive flux. The rapid decay of ^{210}Pb toward local secular equilibrium with ^{226}Ra in a loose sense “buffers” the diffusive fluxes against variations in diffusivity. We performed simulations in which the diffusion coefficient for Pb was factor of ten larger or smaller than the value given in Table 1. This range of diffusion coefficients for Pb is considerably greater than the estimated uncertainty in D_{Pb} ; the values determined by Cherniak (2001) for clinopyroxene crystals with a wide range of composition span about an order of magnitude under the conditions of interest. For “old” clinopyroxene beginning in internal secular equilibrium, increasing D_{Pb} by a factor of ten decreases the (^{210}Pb)/(^{226}Ra) activity ratio of the melt following diffusive interaction, and decreasing D_{Pb} by the same factor increases the activity ratio slightly to 0.79. For “young” clinopyroxene initially in partitioning equilibrium with the melt, increasing or decreasing D_{Pb} by a factor of ten changes the (^{210}Pb)/(^{226}Ra) activity ratio of the melt from 0.73 to 0.63 or 0.84, respectively, after 100 years of interaction. The diffusivity of Ra in clinopyroxene is much less well known than the value for Pb, having been estimated based on a model for the dependence on ionic radius (Van Orman et al., 2001; Saal and Van Orman, 2004), and therefore we examined an even wider range of variation in D_{Ra} . Increasing or decreasing D_{Ra} by a factor of 100 changes the (^{210}Pb)/(^{226}Ra) activity ratio of the melt by only a few percent relative, except when the clinopyroxene is “old” and D_{Ra} is reduced by a factor of 100. In this case a small excess in ^{210}Pb develops in the melt, with (^{210}Pb)/(^{226}Ra) = 1.13 after 100 years of interaction.

Varying the grain size is equivalent to varying the diffusivities of all species simultaneously; increasing the grain size by a factor of two is equivalent to reducing the diffusion coefficients by a factor of four. Changing the grain radius has an influence on the magnitude of the ^{210}Pb – ^{226}Ra fractionation, but not on the direction. A ^{210}Pb deficit in the melt develops regardless of the grain size. Increasing the grain size by a factor of two increases the (^{210}Pb)/(^{226}Ra) activity ratio by ~0.1 after 100 years of interaction, whether the clinopyroxene is “old” or “young”, and decreasing the grain size decreases the activity ratio by a similar factor.

From the simple simulations above, two important conclusions can be drawn regarding the interaction between clinopyroxene and melt:

- (1) Interaction with clinopyroxene leads to a decrease in the (^{210}Pb)/(^{226}Ra) ratio of the melt, which is similar in magnitude whether the clinopyroxene is “young” or “old”; and
- (2) Chemical disequilibrium between the mineral and melt is not a requirement for generating ^{210}Pb – ^{226}Ra fractionation; ^{210}Pb deficits in the examples shown above are generated in the absence of trace element disequilibrium between the clinopyroxene and

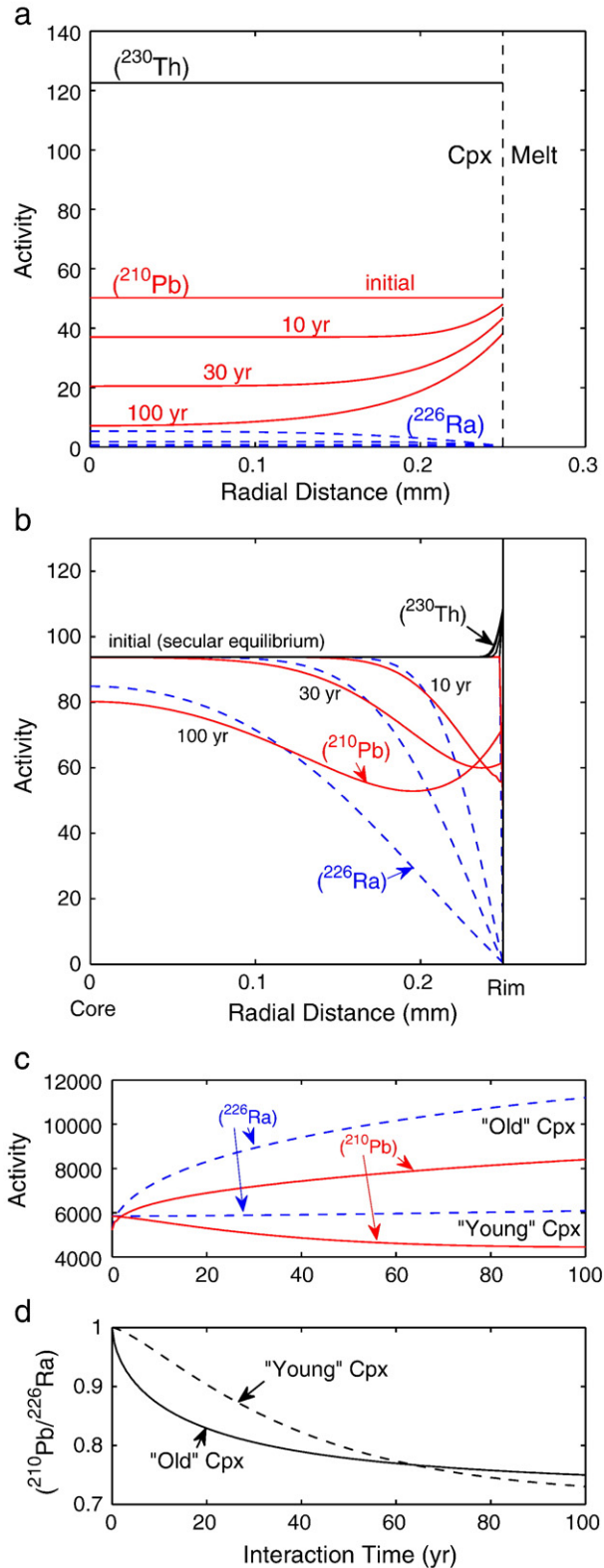


Fig. 1. Simulation results for diffusive exchange with simultaneous radioactive decay in clinopyroxene-melt systems containing 1% melt that is in trace element (^{238}U) partitioning equilibrium with the clinopyroxene and is initially in secular equilibrium. In (a) the intermediate daughters within the clinopyroxene also begin in partitioning equilibrium with the melt (“young” cpx). Radial activity profiles across the clinopyroxene grain are shown after 10, 30 and 100 years of diffusive exchange with the melt. In (b) the intermediate daughters within the clinopyroxene are initially in secular equilibrium with ^{238}U (“old” cpx), and thus far from partitioning equilibrium with the melt. Panels (c) and (d) show ^{210}Pb and ^{226}Ra activities (in arbitrary units; the absolute values have no bearing on the model results), and the (^{210}Pb)/(^{226}Ra) activity ratio in the melt, respectively, as functions of the diffusive interaction time. The activities of ^{210}Pb and ^{226}Ra in the clinopyroxene and the melt follow different paths depending on the initial condition, but in both cases the (^{210}Pb)/(^{226}Ra) activity ratio evolves to a similar value after ~100 years of diffusive interaction.

melt, resulting instead from the decay of ^{210}Pb toward secular equilibrium with ^{226}Ra within the clinopyroxene.

3.2. Melt-plagioclase interaction

Diffusive exchange between melt and plagioclase was simulated for the same two end-member initial conditions described above for

clinopyroxene, with the same melt fraction (1%) and grain radius (0.25 mm). The results are shown in Fig. 2. Melt-plagioclase interaction is different from melt-clinopyroxene interaction mainly in that Pb and Ra are more compatible than Th and U in plagioclase. Lead diffusion in plagioclase is also an order of magnitude faster than in clinopyroxene. Beginning from either of the initial conditions, “partitioning equilibrium” or “secular equilibrium”, the melt develops a $(^{210}\text{Pb})/(^{226}\text{Ra})$ activity ratio <0.2 after 100 years of interaction with plagioclase (Fig. 2d). The major difference between the two examples is that the ^{210}Pb deficit develops much more rapidly when the plagioclase is “old” and initially in internal secular equilibrium. In this “secular equilibrium” case, ^{210}Pb and ^{226}Ra initially have the same activities as ^{238}U and thus have concentrations in plagioclase far below their values at partitioning equilibrium (Fig. 2b). They diffuse in from the melt to bring them closer to partitioning equilibrium, with ^{210}Pb being absorbed from the melt more rapidly due to its larger diffusion coefficient, and larger (initial) concentration gradient. When the plagioclase is “young” and in partitioning equilibrium with the melt initially, ^{210}Pb and ^{226}Ra are also drawn from the melt into the plagioclase, in this case due to the decay of each toward secular equilibrium with its predecessor within the mineral interior. The uptake of these nuclides from the melt is controlled primarily by their rates of decay. As with clinopyroxene-melt interaction, after several decades the ^{210}Pb deficit that develops in the melt is nearly the same regardless of the initial condition, and this deficit develops without any chemical disequilibrium between the plagioclase and melt. For the examples considered here, where the melt fraction is 1%, the ^{210}Pb deficit is significantly greater when the melt interacts with plagioclase. The primary reason is that Pb and Ra have much larger partition coefficients in plagioclase than in clinopyroxene, which gives plagioclase more leverage on the activity ratios in the melt.

As in the clinopyroxene-melt systems considered above, the results are not highly sensitive to variations in the diffusion coefficients. The $(^{210}\text{Pb})/(^{226}\text{Ra})$ activity ratio in the melt is less than or equal to 0.15 after one hundred years of plagioclase-melt interaction, even if D_{Pb} is varied by a factor of ten in either direction or D_{Ra} is varied by a factor of one hundred in either direction. Varying the grain size by a factor of two in either direction changes the $(^{210}\text{Pb})/(^{226}\text{Ra})$ activity ratio by less than 0.02 after 100 years of interaction, whether the plagioclase is “old” or “young”.

3.3. Melt-gabbro interaction and the influence of relative melt enrichment

Here we consider more complicated scenarios in which a cumulate consisting of both clinopyroxene and plagioclase interacts with melts that are enriched or depleted in incompatible trace elements relative to a melt in equilibrium with the cumulate minerals. Similar scenarios were modeled by Van Orman et al. (2006), but without considering ^{210}Pb . The gabbro crystallizes in partitioning equilibrium with an average MORB melt and continues to interact with fresh batches of the same melt until steady state distributions of ^{210}Pb and ^{226}Ra in plagioclase and clinopyroxene are established. The average MORB melt is then replaced by a more enriched or more depleted melt, and the resulting diffusive exchange is simulated for a period of 100 years.

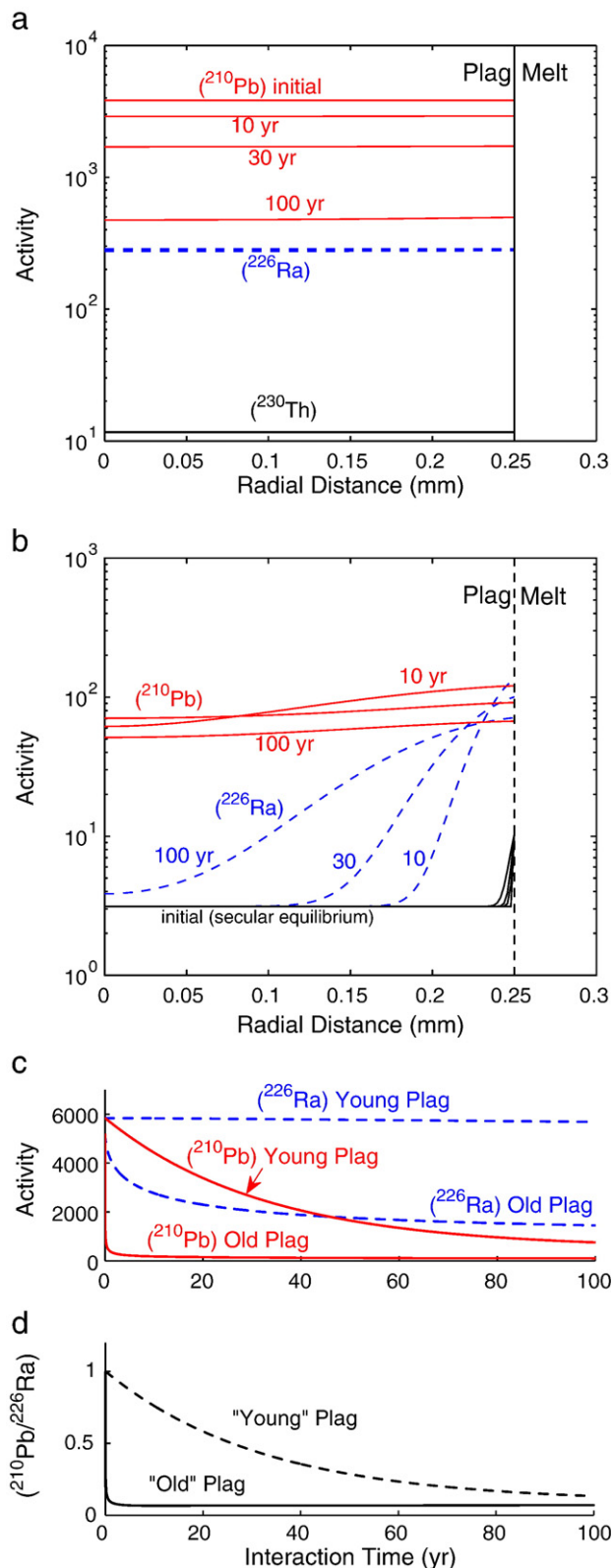


Fig. 2. Simulation results for plagioclase-melt systems with 1% melt, with initial conditions analogous to those shown in Fig. 1 for clinopyroxene-melt systems. In (a) the intermediate daughters in the plagioclase are initially in partitioning equilibrium with the melt (“young” plagioclase), and radial activity profiles across the plagioclase grain are shown after 10, 30 and 100 years of diffusive exchange with the melt. In (b) the intermediate daughters within the plagioclase are initially in secular equilibrium with ^{238}U (“old” plagioclase). Panels (c) and (d) show ^{210}Pb and ^{226}Ra activities (in arbitrary units), and the $(^{210}\text{Pb})/(^{226}\text{Ra})$ activity ratio in the melt, respectively, as functions of the diffusive interaction time. As in the clinopyroxene-melt system, the $(^{210}\text{Pb})/(^{226}\text{Ra})$ activity ratio in the melt evolves toward a similar value beginning from the two very different initial conditions.

When a relatively depleted melt is introduced to a gabbroic cumulate (Fig. 3a), ^{226}Ra diffuses out of the minerals and its activity in the melt thus increases. ^{230}Th also diffuses from the minerals to the melt, but much more slowly; as a result the melt develops a high $(^{226}\text{Ra})/(^{230}\text{Th})$ activity ratio. In contrast to the other nuclides, ^{210}Pb maintains an almost constant activity in the depleted melt. The melt is depleted in ^{210}Pb compared to the melt that crystallized the gabbro, and if decay were neglected it would diffuse rapidly into the melt, thus increasing its concentration. However, as illustrated in the simpler examples described above, this tendency to diffuse from the minerals into the melt is countered by the decay of ^{210}Pb toward secular equilibrium with ^{226}Ra within the plagioclase. This draws down the ^{210}Pb activity near the plagioclase rim and keeps the ^{210}Pb activity in the melt almost constant. With ^{226}Ra in the melt rising, this results in a ^{210}Pb deficit in the melt.

For an enriched melt (Fig. 3b) the behavior is somewhat similar to the simpler case shown in Fig. 2b. Plagioclase absorbs both ^{226}Ra and ^{210}Pb from the melt, ^{210}Pb at a greater rate because it diffuses more rapidly, and because its activity in the plagioclase is drawn down by decay toward (^{226}Ra) . Clinopyroxene also removes ^{210}Pb from the melt in preference to ^{226}Ra , but plagioclase has the dominant influence on the activity ratio due to its much greater capacity for absorbing Pb and

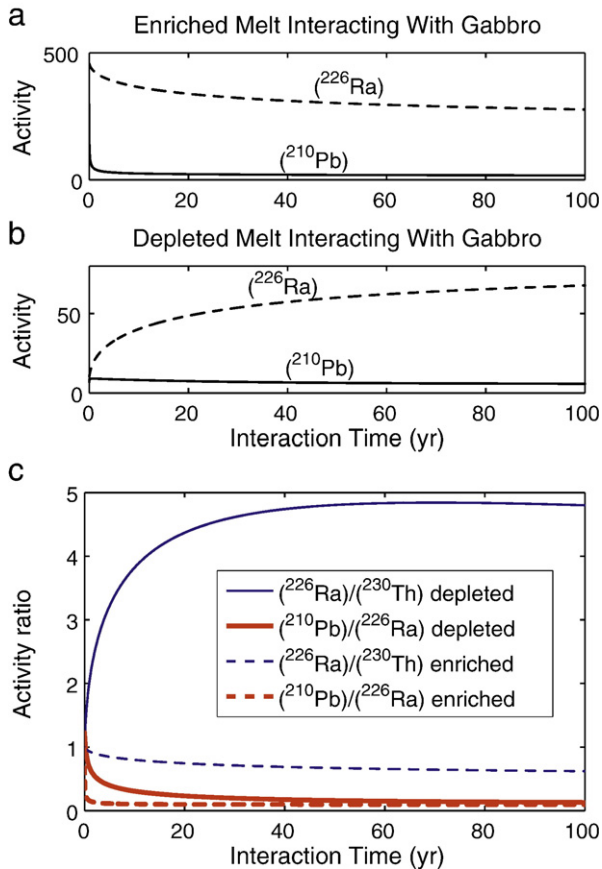


Fig. 3. Simulation results for gabbro–melt systems with 1% melt. The gabbro consists of 40% clinopyroxene, 30% plagioclase and 30% olivine and begins with daughter activity profiles that have reached a steady state during continuous interaction with fresh batches of an average MORB melt. Panels (a) and (b) show the ^{210}Pb and ^{226}Ra activities (in arbitrary units) in enriched and depleted melts, respectively, during diffusive interaction with the gabbro. Panel (c) shows the $(^{226}\text{Ra})/(^{230}\text{Th})$ and $(^{210}\text{Pb})/(^{226}\text{Ra})$ activity ratios in the enriched and depleted melts as functions of the diffusive interaction time. The $(^{226}\text{Ra})/(^{230}\text{Th})$ activity ratio after 100 years of interaction depends strongly on the depletion or enrichment of the melt relative to the gabbro, with depleted melts acquiring large ^{226}Ra excesses and enriched melts acquiring small ^{226}Ra deficits. In contrast, ^{210}Pb deficits are produced in both enriched and depleted melts during interaction with the gabbro, with each melt reaching a similar $(^{210}\text{Pb})/(^{226}\text{Ra})$ activity ratio after 100 years of interaction.

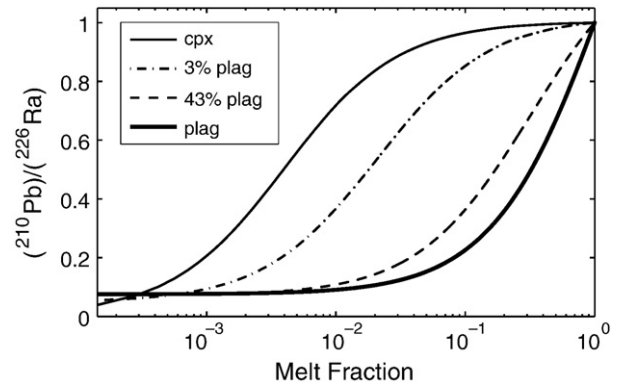


Fig. 4. Influence of melt fraction on the $(^{210}\text{Pb})/(^{226}\text{Ra})$ activity ratio of the melt after diffusive exchange with clinopyroxene, plagioclase, and clinopyroxene-plagioclase mixtures (with 3% and 43% plagioclase). The plotted activity ratios are the steady-state values in the melt, which are achieved after 500 years of diffusive interaction between the melt and cumulate minerals with spherical radii of 0.25 mm.

Ra. The enriched melt rapidly develops a ^{210}Pb deficit, which is very close to the deficit that develops in the depleted melt after 100 years of interaction with the same gabbro. The only substantial difference in result between the enriched and depleted cases is the rate at which the $(^{210}\text{Pb})/(^{226}\text{Ra})$ activity ratio changes during diffusive interaction. When the melt is relatively enriched, $(^{210}\text{Pb})/(^{226}\text{Ra})$ falls very steeply and reaches a near-steady value within a few years; when the melt is depleted, $(^{210}\text{Pb})/(^{226}\text{Ra})$ falls more gradually, over a few decades (Fig. 3c).

Why does the $(^{226}\text{Ra})/(^{230}\text{Th})$ ratio of the melt depend strongly on its enrichment or depletion relative to the gabbro, while the $(^{210}\text{Pb})/(^{226}\text{Ra})$ ratio, after several decades of interaction, does not? For ^{226}Ra , chemical disequilibrium between minerals and melt provides the primary driving force for diffusion; on the timescale of interest, decay does not provide a strong driving force because the decay constant for ^{226}Ra is fairly small. The much more rapid decay of ^{210}Pb provides a strong control on its diffusive exchange between minerals and melt. Decay within plagioclase and clinopyroxene provides an internal sink for ^{210}Pb that enhances its diffusive uptake from an enriched melt, and counteracts its diffusive loss to a depleted melt. ^{210}Pb attains a near steady state with ^{226}Ra within one hundred years, whereas the $(^{226}\text{Ra})/(^{230}\text{Th})$ ratio continues to evolve for a much longer time.

3.4. Influence of melt–rock ratio

The magnitude of $(^{210}\text{Pb})/(^{226}\text{Ra})$ disequilibrium in the melt during diffusive interaction with plagioclase and/or clinopyroxene depends significantly on the fraction of melt in the system. The smaller the melt fraction, and the larger the solid/melt partition coefficients, the more leverage the minerals have on the activity ratio of the melt. Simulations were performed over a large range of melt fraction for melts interacting with clinopyroxene, plagioclase, or mixtures of both minerals, with results shown in Fig. 4. Each curve shows $(^{210}\text{Pb})/(^{226}\text{Ra})$ in the melt after 500 years of interaction, at which time a steady state has been established and the activity ratio is independent of the initial conditions. At very small melt fractions, for the cpx–melt and plag–melt systems, the $(^{210}\text{Pb})/(^{226}\text{Ra})$ activity ratio approaches the inverse ratio of the mineral/melt partition coefficients; i.e. as $F \rightarrow 0$, $(^{210}\text{Pb})/(^{226}\text{Ra}) \rightarrow K_{\text{Ra}}^{\text{min}/\text{melt}}/K_{\text{Pb}}^{\text{min}/\text{melt}}$. Melt interacting with clinopyroxene approaches this limit only at very small melt fractions, $\ll 10^{-4}$, because of its small partition coefficients for Pb and Ra, which give it strong leverage on the melt, and the capability of inducing large ^{210}Pb deficits, only at small melt fractions. Melts interacting with plagioclase, however, maintain a $(^{210}\text{Pb})/(^{226}\text{Ra})$ activity ratio near the limiting value at melt fractions as high as 1%, and have significant ^{210}Pb deficits even at very large melt

fractions (>50%). Plagioclase has a much greater capacity than clinopyroxene to induce $(^{210}\text{Pb})/(^{226}\text{Ra})$ disequilibria in the melt at large melt fractions because of its higher partition coefficients for Pb and Ra.

With reference to Fig. 4, two important points can be made regarding the influence of diffusive exchange with crustal cumulates on $(^{210}\text{Pb})/(^{226}\text{Ra})$ disequilibria.

- 1) The influence of plagioclase on $(^{210}\text{Pb})/(^{226}\text{Ra})$ disequilibria is generally much larger than the influence of clinopyroxene. Interaction with plagioclase-bearing rocks at any point during a melt's ascent toward the surface may rapidly overprint $(^{210}\text{Pb})/(^{226}\text{Ra})$ disequilibria produced by interaction with clinopyroxene during melt–wehrlite interaction, melt–lherzolite interaction, or mantle melting.
- 2) Plagioclase may induce significant $(^{210}\text{Pb})/(^{226}\text{Ra})$ disequilibrium not only during melt percolation through cumulates at low porosities, but possibly also during magma chamber processes, where the melt fraction is large. For example, the liquid in a magma with 20% plagioclase phenocrysts would have a steady-state $(^{210}\text{Pb})/(^{226}\text{Ra})$ activity ratio of ~ 0.89 .

4. Discussion

4.1. Origin of a negative correlation between $(^{210}\text{Pb})/(^{226}\text{Ra})$ and $(^{226}\text{Ra})/(^{230}\text{Th})$ in MORB

An important feature of the Rubin et al. (2005) data set for mid-ocean ridge basalts is a negative correlation between $(^{210}\text{Pb})/(^{226}\text{Ra})$ and $(^{226}\text{Ra})/(^{230}\text{Th})$. The samples cover a wide geographic range, from the Juan de Fuca fracture zone to the southern EPR, suggesting that this correlation may have global significance. Saal and Van Orman (2004) and Van Orman et al. (2006) found that diffusive interaction of relatively enriched and depleted melts with wehrlite, gabbro or troctolite cumulates (originally crystallized from a melt intermediate in composition) could produce a negative correlation between $(^{226}\text{Ra})/(^{230}\text{Th})$ and $(^{230}\text{Th})/(^{238}\text{U})$. However, a negative correlation between $(^{210}\text{Pb})/(^{226}\text{Ra})$ and $(^{226}\text{Ra})/(^{230}\text{Th})$ does not arise from simple interaction of variably enriched melts with plagioclase- or clinopyroxene-bearing cumulates under the same conditions. Diffusive exchange with a cumulate intermediate in composition leads to low $(^{226}\text{Ra})/(^{230}\text{Th})$ in a relatively enriched melt and high $(^{226}\text{Ra})/(^{230}\text{Th})$ in a relatively depleted melt, but both melts have similar ^{210}Pb deficits after one hundred years of interaction (Fig. 3c). Thus, no significant correlation between $(^{210}\text{Pb})/(^{226}\text{Ra})$ and $(^{226}\text{Ra})/(^{230}\text{Th})$ would be expected if the interaction time is ~ 100 years or more. For significantly shorter interaction times, a relatively depleted melt would acquire a smaller deficit in ^{210}Pb than a relatively enriched melt (Fig. 3c), leading to a positive rather than a negative correlation between $(^{210}\text{Pb})/(^{226}\text{Ra})$ and $(^{226}\text{Ra})/(^{230}\text{Th})$. A negative correlation could be produced if there were systematic differences in the porosity, cumulate mineralogy, or residence time for melts on either end of the observed correlation. For example, the interaction of relatively enriched melts at higher porosity or velocity, or with wehrlite rather than gabbroic or troctolitic cumulates, would lead to less ^{210}Pb – ^{226}Ra fractionation and smaller ^{210}Pb deficits in the melts.

The Rubin et al. (2005) data set for MORB shows correlations not only between $(^{210}\text{Pb})/(^{226}\text{Ra})$ and $(^{226}\text{Ra})/(^{230}\text{Th})$ but between ^{210}Pb deficits and various geochemical indicators of magmatic differentiation, including Mg# and various compatible element ratios. The basalts with the smallest ^{210}Pb deficits are more differentiated than their counterparts with larger ^{210}Pb deficits. As Rubin et al. (2005) suggested, these trends can be explained by mixing between a young melt with high ^{226}Ra excess melt and a relatively large ^{210}Pb deficit, and an older melt, with lower ^{226}Ra excess, which has lost its ^{210}Pb deficit due to decay. In this model, the ^{210}Pb deficits and ^{226}Ra excesses are

created prior to magmatic differentiation, and the negative correlation between them results from a systematic difference in “aging” between the basalts with higher and lower ^{226}Ra excesses, during melt transport and/or magma chamber differentiation. Rubin et al. (2005) suggested that the ^{210}Pb deficits (and ^{226}Ra excesses) were created during mantle melting, but the model applies equally well if these are produced in the crust by diffusive interaction with cumulates, prior to their accumulation and mixing in magma chambers.

4.2. ^{210}Pb excesses

Although most young volcanic samples that exhibit ^{210}Pb – ^{226}Ra disequilibria have ^{210}Pb deficits, some seamount (Rubin et al., 2005) and subduction zone lavas (e.g. Turner et al., 2004) have ^{210}Pb excesses. Rubin et al. (2005) noted that ^{210}Pb excesses are difficult to produce by mantle melting; we have found that they are also difficult to produce during diffusive interactions in the crust. When melt that is depleted in incompatible trace elements interacts with gabbroic cumulates that crystallized from a more enriched melt, there is a very short period (\sim two months) during which a small excess in ^{210}Pb develops in the melt, due to the more rapid diffusion of Pb from the plagioclase, relative to Ra. However, it is the relatively depleted samples in the Rubin et al. (2005) data set that have the largest ^{210}Pb deficits; the samples with ^{210}Pb excesses are somewhat more enriched in trace elements. Diffusive interaction with plagioclase or clinopyroxene thus seems unlikely to explain ^{210}Pb excesses in natural samples.

Plagioclase accumulation has been suggested as a hypothetical explanation for ^{210}Pb excesses (Rubin et al., 1989, 2005). When plagioclase, or clinopyroxene, crystallize from or diffusively exchange U-series isotopes with a melt, these minerals develop an excess of ^{210}Pb that is complementary to the ^{210}Pb deficit that develops in the melt. Dissolution of either plagioclase or clinopyroxene might, therefore, produce excess ^{210}Pb in a melt. However, the dissolution would have to be quite fast if the melt is to avoid simultaneous diffusive exchange with the minerals, which would arrest or erase the development of a ^{210}Pb excess in the melt. Because significant ^{210}Pb deficits develop quite rapidly during diffusive interaction with plagioclase or gabbroic cumulates, often on timescales significantly less than a year, this mechanism for generating ^{210}Pb excesses also seems rather unlikely.

Another way ^{210}Pb excesses may be produced is by the accumulation of ^{222}Rn -enriched vapor bubbles that diffusively exchange ^{210}Pb with the melt (Turner et al., 2004). ^{222}Rn , a noble gas and the immediate daughter of ^{226}Ra , will partition strongly into any gas phase that exsolves as a magma ascends. If the vapor bubbles rise significantly faster than the magma, they will carry with them excess ^{222}Rn which decays over a few days to ^{210}Pb . Diffusion of ^{210}Pb from the bubbles to the melt may then produce excess ^{210}Pb in the melt. In this way, magmas that have experienced a net loss of vapor may develop a ^{210}Pb deficit, and those that have experienced a net accumulation of gas bubbles (presumably at higher levels within the magma plumbing system) may develop a ^{210}Pb excess. Such a bubble accumulation process seems a plausible hypothesis for the ^{210}Pb excesses observed in some subduction zone lavas (Turner et al., 2004) and at Axial seamount (Rubin et al., 2005).

4.3. ^{210}Pb deficits in subduction zone lavas

Historical lavas from subduction zones commonly have substantial ^{210}Pb deficits, with $(^{210}\text{Pb})/(^{226}\text{Ra})$ ratios as low as 0.24 (Turner et al., 2004). The lack of correlation of these deficits with geochemical indicators of fluid addition or partial melting, and the presence at some volcanoes of lavas with both ^{210}Pb excesses and ^{210}Pb deficits, suggest that degassing has played a role in generating the ^{210}Pb – ^{226}Ra disequilibria (Turner et al., 2004). Gauthier and Condomines (1999) presented a model for the evolution of $(^{210}\text{Pb})/(^{226}\text{Ra})$ during degassing of ^{222}Rn from of a magma, and showed that significant

^{210}Pb deficits could be produced if ^{222}Rn loss is efficient, the magma recharge rate is not very high, and the degassing duration is sufficiently long relative to the timescale of ^{210}Pb decay. Turner et al. (2004) applied this model to an extensive data set for subduction zone lavas and found that to produce the lowest observed (^{210}Pb)/(^{226}Ra) activity ratios by degassing alone requires continuous degassing for at least 47 years, assuming perfect ^{222}Rn loss and no magma recharge. Although degassing likely plays an important role in ^{210}Pb – ^{226}Ra fractionation in subduction settings, as indicated by the presence of ^{210}Pb excess in some lavas, the results presented in this paper suggest caution in interpreting ^{210}Pb deficits in terms of degassing alone. Diffusive interaction of melts with plagioclase cumulates or phenocrysts is capable of generating ^{210}Pb deficits on much shorter timescales than can be achieved by degassing. By this mechanism, ^{210}Pb deficits can be produced even if degassing is inefficient and magma recharge rates are high. Hence, large ^{210}Pb deficits are not necessarily indicative of long-term, continuous degassing from a magma chamber with sluggish magma recharge.

5. Conclusions

Diffusive exchange with cumulate minerals in the crust may exert a strong control on ^{230}Th – ^{226}Ra – ^{210}Pb disequilibria in basaltic melts. Diffusive fractionation between ^{226}Ra and ^{230}Th depends strongly on the trace element disequilibrium between the melt and cumulate, with ^{226}Ra excesses developing in the melt under many circumstances but ^{226}Ra deficits also possible (Saal and Van Orman, 2004; Van Orman et al., 2006). In contrast, diffusive exchange with clinopyroxene and/or plagioclase cumulates is expected to produce ^{210}Pb deficits in the melt in virtually every circumstance. The contrasting behavior of ^{226}Ra and ^{210}Pb results mainly from the difference in their rates of decay. For ^{226}Ra , decay is relatively slow and diffusive exchange in many cases is driven by chemical disequilibrium between the melt and cumulate. Diffusive exchange of ^{210}Pb , on the other hand, tends to be governed by its rapid decay toward secular equilibrium with ^{226}Ra .

Plagioclase in the crust has a greater capacity to fractionate ^{210}Pb from ^{226}Ra than any silicate mineral present during mantle melting. Diffusive exchange with plagioclase leads to significant ^{210}Pb deficits in the melt even after very short interaction times (less than a year) and even when the melt fraction is above 50%. The ^{210}Pb deficits found in mid-ocean ridge basalts can be explained by diffusive exchange with plagioclase- or clinopyroxene-bearing cumulates, and do not require melt to be transported rapidly (in less than 100 years) to the surface from distributed grain-scale porous networks in the mantle. In subduction zones, ^{210}Pb deficits do not necessarily imply long-term continuous degassing from magma chambers with low rates of recharge, but may result in part from diffusive interactions with minerals in the crust.

Acknowledgments

We would like to thank Ken Rubin and Aaron Pietruszka for constructive reviews and Rick Carlson for helpful editorial suggestions. This work was supported by the National Science Foundation under Grant No. 0337125.

References

- Bergmanis, E.C., Sinton, J., Rubin, K.H., 2007. Recent eruptive history and magma reservoir dynamics on the southern East Pacific Rise at $17^{\circ}30'\text{S}$. *Geochem. Geophys. Geosys.* 8, Q12006.
- Bindeman, I.N., Davis, A.M., Drake, M.J., 1998. Ion microprobe study of plagioclase-basalt partition experiments at natural concentration levels of trace elements. *Geochim. Cosmochim. Acta* 62, 1175–1193.
- Bindeman, I.N., Davis, A.M., Drake, M.J., 2007. Erratum to “Ion microprobe study of plagioclase-basalt partition experiments at natural concentration levels of trace elements”. *Geochim. Cosmochim. Acta* 71, 2414.
- Blundy, J.D., Wood, B.J., 2003. Mineral-melt partitioning of uranium, thorium and their daughters. *Rev. Mineral. Geochem.* 52, 59–118.
- Bourdon, B., Sims, K.W., 2003. U-series constraints on intraplate basaltic magmatism. *Rev. Mineral. Geochem.* 52, 215–253.
- Cherniak, D.J., 1995. Diffusion of lead in plagioclase and K-feldspar: an investigation using Rutherford Backscattering and Resonant Nuclear Reaction Analysis. *Contrib. Mineral. Petrol.* 120, 358–371.
- Cherniak, D.J., 1998. Pb diffusion in clinopyroxene. *Chem. Geol.* 150, 105–117.
- Cherniak, D.J., 2001. Pb diffusion in Cr diopside, augite, and enstatite, and consideration of the dependence of cation diffusion in pyroxene on oxygen fugacity. *Chem. Geol.* 177, 381–397.
- Condomines, M., Tanguy, J.-C., Michaud, V., 1995. Magma dynamics at Mt. Etna: constraints from U–Th–Ra–Pb radioactive disequilibria and Sr isotopes in historical lavas. *Earth Planet. Sci. Lett.* 132, 25–41.
- Dunn, R.A., Forsyth, D.W., 2003. Imaging the transition between the region of mantle melt generation and the crustal magma chamber beneath the southern East Pacific Rise with short-period Love waves. *J. Geophys. Res.* 108, 2352.
- Dunn, R.A., Toomey, D.R., Solomon, S.C., 2000. Three-dimensional seismic structure and physical properties of the crust and shallow mantle beneath the East Pacific Rise at $9^{\circ}30'\text{N}$. *J. Geophys. Res.* 105, 23537–23555.
- Dunn, R.A., Toomey, D.R., Detrick, R.S., Wilcock, W.S., 2001. Continuous mantle melt supply beneath an overlapping spreading center on the East Pacific Rise. *Science* 291, 1955–1958.
- Gauthier, P.J., Condomines, M., 1999. Pb–210–Ra–226 radioactive disequilibria in recent lavas and radon degassing: inferences on the magma chamber dynamics at Stromboli and Merapi volcanoes. *Earth Planet. Sci. Lett.* 172, 111–126.
- Gill, J.B., Williams, R.W., 1990. Th isotope and U-series studies of subduction-related volcanic rocks. *Geochim. Cosmochim. Acta* 54, 1427–1442.
- Hart, S.R., 1993. Equilibration during mantle melting: a fractal tree model. *Proc. Natl. Acad. Sci. USA* 90, 11914–11918.
- Kelemen, P.B., Hirth, G., Shimizu, N., Spiegelman, M., Dick, H.J.B., 1997. A review of melt migration processes in the adiabatically upwelling mantle beneath oceanic spreading ridges. *Philos. Trans. R. Soc. Lond. A* 355, 283–318.
- Lundstrom, C.C., 2003. Uranium-series disequilibria in mid-ocean ridge basalts: observations and models of basalt genesis. *Rev. Mineral. Geochem.* 52, 175–212.
- Lundstrom, C.C., Shaw, H.F., Ryerson, F.J., Phinney, D.L., Gill, J.B., Williams, Q., 1994. Compositional controls on the partitioning of U, Th, Ba, Pb, Sr and Zr between clinopyroxene and haplobasaltic melts: implications for uranium series disequilibria in basalts. *Earth Planet. Sci. Lett.* 128, 407–423.
- McKenzie, D., 2000. Constraints on melt generation and transport from U-series activity ratios. *Chem. Geol.* 162, 81–94.
- Miller, S.A., Burnett, D.S., Asimow, P.D., Phinney, D.L., Hutcheon, I.D., 2007. Experimental study of radium partitioning between anorthite and melt at 1 atm. *Am. Mineral.* 92, 1535–1538.
- Oversby, V.M., Gast, P.W., 1968. Lead isotope compositions and uranium decay series disequilibrium in recent volcanic rocks. *Earth Planet. Sci. Lett.* 5, 199–206.
- Reagan, M.K., Turner, S., Legg, M., Sims, K.W.W., Hards, V.L., 2008. ^{238}U - and ^{232}Th -decay series constraints on the timescales of crystal fractionation to produce the phonolite erupted in 2004 near Tristan da Cunha, South Atlantic Ocean. *Geochim. Cosmochim. Acta* 72, 4367–4378.
- Richardson, C., McKenzie, D., 1994. Radioactive disequilibria from 2D models of melt generation by plumes and ridges. *Earth Planet. Sci. Lett.* 128, 425–437.
- Rubin, K.H., Macdougall, J.D., 1989. Submarine magma degassing and explosive volcanism at Madonald (Tamariki) Seamount. *Nature* 341, 50–52.
- Rubin, K.H., Wheller, G.E., Tanzer, M.O., Macdougall, J.D., Varne, R., Finkel, R., 1989. U-238 decay series systematics of young lavas from Batur Volcano, Sunda Arc. *J. Volcanol. Geotherm. Res.* 38, 215–226.
- Rubin, K.H., van der Zander, I., Smith, M.C., Bergmanis, E.C., 2005. Minimum speed limit for ocean ridge magmatism from ^{210}Pb – ^{226}Ra – ^{230}Th disequilibria. *Nature* 437, 534–538.
- Saal, A.E., Van Orman, J.A., 2004. The ^{226}Ra enrichment in oceanic basalts: evidence for diffusive interaction processes within the crust–mantle transition zone. *Geochem. Geophys. Geosys.* 5 Art. No. Q02008.
- Salter, V.J.M., Longhi, J.E., Bizimis, M., 2002. Near mantle solidus trace element partitioning at pressures up to 3.4 GPa. *Geochem. Geophys. Geosys.* 3 Art. No. 1038.
- Sigmarrsson, O., 1996. Short magma chamber residence time at an Icelandic volcano inferred from U-series disequilibria. *Nature* 382, 440–442.
- Sigmarrsson, O., Condomines, M., Bachèlery, P., 2005. Magma residence time beneath the Piton de la Fournaise Volcano, Reunion Island, from U-series disequilibria. *Earth Planet. Sci. Lett.* 234, 223–234.
- Sims, K.W.W., Hart, S.R., Reagan, M.K., Blusztajn, J., Staudigel, H., Sohn, R.A., Layne, G.D., Ball, L.A., Andrews, J., 2008. ^{238}U – ^{230}Th – ^{226}Ra – ^{210}Pb – ^{210}Po , ^{232}Th – ^{228}Ra and ^{235}U – ^{231}Pa constraints on the ages and petrogenesis of Vaialulu'u and Malumalu Lavas, Samoa. *Geochem. Geophys. Geosys.* 9 Art. No. Q04003.
- Turner, S., Black, S., Berlo, K., 2004. Pb–210–Ra–226 and Ra–228–Th–232 systematics in young arc lavas: implications for magma degassing and ascent rates. *Earth Planet. Sci. Lett.* 227, 1–16.
- Van Orman, J.A., Grove, T.L., Shimizu, N., 1998. Uranium and thorium diffusion in diopside. *Earth Planet. Sci. Lett.* 160, 505–519.
- Van Orman, J.A., Grove, T.L., Shimizu, N., 2001. Rare earth element diffusion in diopside: influence of temperature, pressure and ionic radius, and an elastic model for diffusion in silicates. *Contrib. Mineral. Petrol.* 141, 687–703.
- Van Orman, J.A., Saal, A.E., Bourdon, B., Hauri, E.H., 2006. Diffusive fractionation of U-series radionuclides during mantle melting and shallow-level melt-cumulate interaction.
- Zhang, Y., Walker, D., Leshner, C.E., 1989. Diffusive crystal dissolution. *Contrib. Mineral. Petrol.* 102, 492–513.